Published in final edited form as:
Nanomedicine (Lond). 2011 June ; 6(4): 617–630. doi:10.2217/nnm.11.20.

Gold Nanorod-siRNA Induces Efficient *In Vivo* Gene Silencing in the Rat Hippocampus

Adela C. Bonoiu[2], **Earl J. Bergey**[2,3], **Hong Ding**[2], **Rui Hu**[2], **Rajiv Kumar**[2], **Ken-Tye Yong**[2,7], **Paras N. Prasad**[*,2], **Supriya Mahajan**[4], **Kelly E. Picchione**[5], **Arin Bhattacharjee**[5,6], and **Tracey A. Ignatowski**[*,1,5]

[1] Department of Pathology and Anatomical Sciences, School of Medicine and Biomedical Sciences, State University of New York at Buffalo, 3435 Main Street, Buffalo, NY 14214

[2] Institute for Lasers, Photonics, and Biophotonics, State University of New York at Buffalo, 3435 Main Street, Buffalo, NY 14214

[3] Department of Chemistry, School of Arts and Sciences, State University of New York at Buffalo, 3435 Main Street, Buffalo, NY 14214

[4] Department of Medicine, Division of Allergy, Immunology, and Rheumatology, School of Medicine and Biomedical Sciences, State University of New York at Buffalo, 3435 Main Street, Buffalo, NY 14214

[5] Program for Neuroscience, School of Medicine and Biomedical Sciences, State University of New York at Buffalo, 3435 Main Street, Buffalo, NY 14214

[6] Department of Pharmacology and Toxicology, School of Medicine and Biomedical Sciences, State University of New York at Buffalo, 3435 Main Street, Buffalo, NY 14214

[7] School of Electrical and Electronic Engineering, Nanyang Technological University, Nanyang Avenue, Singapore 639798, Singapore

Abstract

Gold nanorods (GNRs), cellular imaging nanoprobes, have been used for drug delivery therapy to immunologically privileged regions in the brain. We demonstrate that nanoplexes formed by electrostatic binding between negatively charged RNA and positively charged GNRs, silence the expression of the target housekeeping gene, glyceraldehyde 3-phosphate dehydrogenase (GAPDH) within the CA1 hippocampal region of the rat brain, without showing cytotoxicity. Fluorescence imaging with siRNA^{Cy3}GAPDH and dark field imaging using plasmonic enhanced scattering from GNRs were used to monitor the distribution of the nanoplexes within different neuronal cell types present in the targeted hippocampal region. Our results show robust nanoplex uptake and slow release of the fluorescent gene silencer with significant impact on suppression of GAPDH gene expression (70% gene silencing, >10 days post-injection). The observed gene knockdown using nanoplexes in targeted regions of the brain opens a new era of drug treatment for neurological disorders.

[*]Corresponding Authors: Tracey A. Ignatowski, Department of Pathology and Anatomical Sciences, School of Medicine and Biomedical Sciences, State University of New York at Buffalo, 206 Farber Hall, 3435 Main St. Buffalo, NY 14214, phone: (716) 829-3102, fax: (716) 829-2086, tai1@buffalo.edu and Paras N. Prasad, Institute for Lasers, Photonics, and Biophotonics, State University of New York at Buffalo, 428 Natural Science Complex, Buffalo, NY 14260, phone: (716) 645-4148, -4147, fax: (716) 645-6945, pnprasad@buffalo.edu.

Keywords

gold nanorods; hippocampus; rat; siRNA; transfection; neurological disorders; dark field; brain

1. Introduction

The field of nanomedicine is rapidly advancing with the development of novel nanoparticle formulations that serve as efficient carriers for diagnostic and therapeutic purposes [1–3]. Nanoparticles were initially used as bioimaging probes and as drug delivery vehicles [1, 4]. Recently, they have been used for *in vitro* delivery of polynucleotides such as plasmid DNA and siRNA, as efficient non-viral vectors in gene therapy [5–7]. They provide a superior gene transfection vector compared to current viral vectors due to the lack of carrier toxicity, immune-mediated injury, and conversion of virus to pathogenic forms [8–10]. Selective gene inhibition by siRNA 'targeted' therapeutics promises the ultimate level of specificity, but siRNA therapeutics are hindered by poor intracellular uptake, limited stability in circulation, and non-specific immune stimulation. In spite of these limitations, therapeutics that are designed to involve RNA interference (RNAi) or gene silencing using siRNA have the potential to provide new ways of imparting therapy to patients [11–15].

Recently, gold nanoparticles (GNPs) and nanorods (GNRs) have been used as probes for *in vivo* and *in vitro* applications due to their low toxicity in biological environments [16–19]. Their surfaces can be modified to contain cationic charges that readily form electrostatic complexes with anionic genetic materials (DNA or RNA) for targeted gene delivery/silencing. Resonant electron oscillations on the surface of noble metal nanoparticles (Au, Ag, Cu) create a surface (Surface Plasmon Resonance, SPR) that greatly enhances the absorption and scattering of light, thereby making these particles well-suited for optical detection/tracking in biological models [5, 7, 9]. In order to confirm both the successful formation of nanoplexes after attaching siRNA molecules on the GNR surface and the stability of this nanocomplex over time, SPR investigations were performed. Our group has developed GNRs coated with cationic polyelectrolytes as multimodal probes with capability for dark-field imaging and for electron microscopy [9, 20]. These GNRs were complexed with siRNA, which stabilized the siRNA, and acted as vectors to deliver the siRNA to cells [21]. More specifically, we have shown that these GNRs can be used as probes for delivering siRNA and silencing the expression of dopamine-and cAMP-regulated phosphoprotein of molecular weight 32 kD (DARPP-32) in dopaminergic neuronal (DAN) cells *in vitro* [22]. We have further shown that GNRs are able to cross the blood-brain barrier and accumulate in the neural tissue [22].

In the current study, we used a fluorescent labeled siRNA against glyceraldehyde 3-phosphate dehydrogenase (GAPDH) that was complexed to GNRs (GNR-GAPDH siRNA^{Cy3}) and stereotaxically injected this nanoplex into the CA1 region of the hippocampus in Sprague-Dawley rats. This study demonstrates that stereotaxic injection of GNR-siRNA into the brain, specifically into the hippocampus can effectively knock-down gene expression with longer localized effects due to sustained release from the nanoparticle surface. These results suggest that a personalized medicine approach can be safely formulated in the near future based on GNR-siRNA nanoplexes as therapeutic agents for patients with neurological disorders and brain tumors [13, 22, 23].

2. Materials and methods

Synthesis of Nanoplexes for siRNA Delivery: Materials

Cetyltrimethylammonium bromide (CTAB), hydrogen tetrachloroaurate(III) trihydrate ($HAuCl_4*3H_2O$), silver nitrate (AgNO3), L-ascorbic acid, glutaraldehyde (50% aqueous solution), and sodium borohydride were purchased from Aldrich. All chemicals were used as received. HPLC-grade water was used in all the experiments. Stock solutions of sodium borohydride and L-ascorbic acid were freshly prepared for each new set of experiments. Poly(3,4-ethylenedioxythiophene)/poly(styrenesulfate) (PEDT/PSS, molecular weight 240,000) and poly(diallyldimethyl ammonium chloride) (PDDAC, 20%) were obtained from Polysciences, Inc.

Nanoplex Synthesis

The GNRs were prepared by the seed-mediated growth method in CTAB surfactant solution. CTAB forms rod-like micelles above its critical micelle concentration (cmc) and therefore forms the template for the subsequent synthesis of GNRs. Following that, the positively charged CTAB-coated GNRs were further coated with two successive layers of polyelectrolytes, (a) the negatively charged PEDT/PSS (20%) and (b) the positively charged PDDAC (20%). This polymeric multilayering was necessary in order to generate positively charged GNRs, yet "masking" the CTAB layer, which is known for its cytotoxicity. The detailed procedures in each step have been described [9,24]. The cationic GNRs were then electrostatically complexed with the siRNA by incubating 9 pmoles of siRNA and 100 μl of GNRs in phosphate-buffered saline (PBS) solution for 4 hr at 37°C. The sample was filter sterilized prior to injection.

For transmission electron microscopy (TEM), transfected cells were fixed as described [3], sectioned (70–100 nm), stained with lead citrate, and viewed with a Tecnai-12 electron microscope (Phillips) at 120 kV. Nanoplex surface charge studies for determining zeta potential of GNRs in the presence and absence of RNA molecules were performed at 25°C using a 90-Plus particle size analyzer (Brookhaven Instrument Corp.).

Animals

Male Sprague-Dawley rats (250–350 g) (Harlan Sprague-Dawley Inc., Indianapolis, IN) were used for all experiments. The rats were housed in Laboratory Animal Facility-accredited pathogen-free quarters at 23 ± 1° C, with access to food and water *ad libitum*. The animals were maintained on a 12 h light/dark cycle. All protocols were approved by the Institutional Animal Care and Use Committee (IACUC) of the University at Buffalo as well as with the guidelines for the ethical treatment of animals established by the National Institute of Health. All efforts were made to ensure minimal animal suffering, as well as to use the minimum number of animals necessary to obtain reproducible results.

Embryonic Dorsal Root Ganglion (DRG) Neurons

Embryonic dorsal root ganglion (DRG) neurons that are commonly used to study neuron function and grow readily in culture were dissected from E15 embryos of Sprague-Dawley rats, and the ganglia were dissociated in trypsin (2.5 mg/ml) (Sigma) for 40 min. Cells were grown on poly-D-lysine (100 μg/ml) and laminin (3 μg/ml) (Sigma) coated coverslips and maintained in serum-free medium containing β-nerve growth factor (NGF, 100 ng/ml, Harlan Biosciences, Indianapolis, IN). The day after plating, cells were treated with 1μM cytosine-β-D-arabinofuranoside, an inhibitor of DNA synthesis, to inhibit growth of non-neuronal cells for 2 days. Neurons were allowed to recover for 2–3 days prior to manipulation [25].

Studies of Nanoplex Distribution In Vitro

The DRG cellular uptake of the nanoplexes GNR-siRNA^{FAM}, siPORT-siRNA^{FAM}, and free siRNA^{FAM} (Cat. No. AM 4650, Ambion, TX) distribution was monitored using dark-field and fluorescence microscopy. The signal from siRNA^{FAM} was acquired using a fluorescence microscope (see section *Confocal and Dark Field Microscopy*) equipped with a 488ex/510em filter, and for acquiring the signal from the nuclear dye Hoechst, a 405ex/460em filter was used. Cell viability was determined by MTT assays [22, 26].

Nanoplex Injection and siRNA-Targeted Knockdown

Animals were anesthetized with an intraperitoneal (i.p.) injection of ketamine (75 mg/kg) and xylazine (10 mg/kg) and were secured on a stereotaxic platform. The stereotaxic coordinates: 3.3 mm posterior to bregma (anterior-posterior); 1.6 mm lateral to the midline (medial-lateral); and 2.8 mm below the dura (dorsal-ventral) were used for injection into the CA1 region of the hippocampus [27]. Briefly, GNR-GAPDH-targeting siRNA^{Cy3} (*Silencer*® Cy™3-Labeled Select siRNA, Cat. No. AM4649, Ambion, Austin, TX), GNR-scrambled siRNA^{Cy3} (*Silencer*® Cy™3-Labeled Negative Control #1 siRNA, Ambion, Cat. No. AM4621), free GAPDH-targeting siRNA^{Cy3} (Ambion), or vehicle (saline) alone were injected into the CA1 region of the right hippocampus. GNRs alone were not injected due to a difference in surface charge as compared to the nanoplex (see **Results 3.1**) [22, 28]. The concentration of GNR-GAPDH-targeting siRNA (500 ng/1 nmol in 6 μl) for injection was based on *in vitro* studies[7, 29]. Each injection occurred at a rate of 0.5 μl/min using a 30 G stainless steel needle on a 10 μl Hamilton syringe, held by the micromanipulator on the stereotaxic apparatus [7]. The needle remained in place for another 3 minutes after the injection to allow for sufficient diffusion. Verification of the injection site was confirmed by gross morphology of the hippocampus at dissection.

Immunofluorescent Staining

The hippocampus was embedded in Tissue-Tek® O.C.T. compound (Finetech, Torreance, CA), snap frozen in liquid nitrogen, and sectioned. Serial sections (10 μm) were collected on StarFrost™ glass slides (Mercedes Medical, Sarasota, FL) and stored at −80°C until stained. Sections on slides were brought to room temperature and fixed in acetone, 10 min at room temperature. Slides were completely dried prior to hydration in 1X PBS at room temperature, 3 times, 5 min each. Non-specific binding of IgGs was blocked with 10% goat serum for 20 min at room temperature. Slides were blotted without washing to remove serum. Sections were incubated with primary antibody for either glial fibrillary acidic protein, mouse monoclonal anti-GFAP (1:30,000, Sigma-Aldrich) or neurofilament-200, mouse monoclonal NF-200 (1:30,000, Sigma), both of which cross-react with rat, 120 min, in 1X PBS/1% bovine serum albumin (BSA) (fraction V)/10% goat serum at room temperature in a humidified chamber. Slides were washed 3 times, 5 min each, in 1X PBS. Sections were incubated with the secondary antibody, goat anti-mouse IgG1-AlexaFluor 647 (1:2,000, Invitrogen), in 1X PBS/1% BSA, 120 min at room temperature in a humidified chamber in the dark. Slides were washed 5 times, 5 min each, in 1X PBS. Sections were incubated with Hoechst nuclear stain (10 μM) for 1 min. Slides were rinsed with 1X PBS, 1X, 5 min. Fluoromount™ aqueous mounting medium with anti-fade properties (Sigma) was added to slides, which were then cover slipped. Slides were stored in the dark at −20°C until analyzed [30].

Confocal and Dark Field Microscopy

The cellular uptake of the GNRs conjugated with GAPDH-siRNA^{Cy3} was visualized using dark-field and confocal microscopy. The light-scattering images were recorded using an upright Nikon Eclipse 800 microscope with a high numerical dark-field condenser (NA

1.20–1.43, oil immersion) and a 100/1.4 NA oil Iris objective (Cfi Plan Fluor). In the dark-field configuration, the condenser delivers a narrow beam of white light from a tungsten lamp, and the high NA oil immersion objective collects only the scattered light from the samples. The dark-field imaging was captured using a QImaging Micropublisher 3.3 RTV color camera. The Qcapture software from the camera manufacturer was used for image acquisition and has a feature for adjusting the white color balance for accurately capturing the color differences in samples. Confocal microscopic images were obtained using a spectral confocal microscope (TCS SP2, Leica Microsystems Semiconductor GmbH) with a HXC PL APO CS 63.0×1.40 oil immersion objective. The DRG neurons transfected with GNR-siRNA^{FAM} used a 488ex/510em filter to acquire the FAM signal, and acquiring the signal from the nuclear dye Hoechst used a 405ex/460em filter. The hippocampal tissue sections taken from rats microinjected with GNR-siRNA^{Cy3} were excited by a pulsed diode laser at 540 nm (PDL800-D, PicoQuant GmbH); photomultiplier tube 1 (PMT1) was set with filter of 550–590 nm [9].

Reflectance Analysis of Nanoplex Distribution

Rat CA1 hippocampal regions were injected with GNR-GAPDH siRNA^{Cy3} nanoplexes (500 ng/1 nmol in 6 μl). Four and 11 days post injection, animals were euthanized and whole brains isolated. Tissue sections (4 μm) were prepared from either whole brain specimen snap-frozen in liquid nitrogen or paraffin-embedded following perfusion fixation (4% paraformaldehyde, 4°C; tissue post-fixed in 30% sucrose in 0.1M phosphate overnight or until tissue sinks). Paraffin sections were deparafffinized in xylene (3 × 5 min), followed by rehydration through a series of graded ethanol (100%, 2 × 3 min; 95, 95, 70, 70%; 2 min each) washes to H_2O. Sections were mounted with aqueous mounting media and coverslipped. Reflectance imagining of the hippocampal sections was performed with confocal microscopy (TCS SP2, Leica Microsystems Semiconductor GmbH, equipped with a HXC PL APO CS 63.0×1.40 oil immersion objective) in reflectance mode [31–33].

RNA Extraction and Quantitative-Real Time-PCR

Upon dissection, the CA1 region and the CA3/dentate gyrus portion of the hippocampus, as well as a portion of the parietal cortex directly over the site of hippocampal injection, were placed into 1 ml RNA*later* solution (Ambion) and stored at −80°C until RNA extraction. Total RNA was extracted by an acid guanidinium-thiocynate-phenol-chloroform method as described using TRIzol reagent (Invitrogen-Life Technologies, Carlsbad, CA) [34]. Real time, quantitative PCR (Q-PCR) was used to quantitate the relative abundance of each mRNA species using specific primers for GAPDH: Forward primer: 5′-accatagcagggacaaggtg-3′; Reverse Primer: 5′-ccagctcactgtcttccaca-3′. Briefly, 10 mg of frozen brain tissue was disintegrated by grinding in the RNA extraction reagent Trizol (Invitrogen, Carlsbad, CA) using a disposable mortar and pestle (Cat # TS4-709 Labsource Inc, Romeoville, IL). RNA concentrations were determined using a Nano-Drop ND-1000 spectrophotometer. Isolated RNA was stored at −80°C. RNA was then reverse transcribed to cDNA using a reverse transcriptase kit (Promega Inc, Madison, WI). Relative abundance of each mRNA species was quantitated by Q-PCR using specific primers for GAPDH and β-actin and the Brilliant® SYBR® green Q-PCR master mix (Stratagene Inc, La Jolla, CA). To provide precise quantification of initialtarget in each PCR reaction, the amplification plot was examined at a point during the early log phase of product accumulation. This was accomplished by assigning a fluorescence threshold above background and determining the time point at which each sample' samplification plot reached the threshold (defined as the thresholdcycle number or C_T). Differences in threshold cycle number were used to quantify the relative amount of PCR target containedwithin each tube. Relative expression of mRNA species was calculated using the comparative C_T method [35, 36]. All data were controlled for quantity of RNA input by performing measurements on an endogenous reference gene,

β-actin. Results on RNA from treated samples were normalized to results obtained on RNA from the control sample. Briefly, the analysis was performed as follows: for each sample, a difference in C_T values (ΔC_T) was calculated for each mRNA by taking the meanC_T of duplicate tubes and subtracting the mean C_T of the duplicatetubes for the reference RNA (β-actin) measured on an aliquot from the same RT reaction. The ΔC_T for the treated sample was then subtracted from the ΔC_T for the untreated control sample to generate a $\Delta\Delta C_T$. The mean of these $\Delta\Delta C_T$ measurements was then used to calculate expression of the test gene relative to the reference gene and normalized to the untreated control as follows: Relative Expression/Transcript Accumulation Index = $2^{-\Delta\Delta CT}$. This calculation assumes that all PCR reactions are working with 100% efficiency. All PCR efficiencies were found to be >95%; therefore, this assumption introduces minimal error into the calculations. Data are the mean ± SD of 3 separate experiments done in duplicate. Statistical significance was determined using ANOVA based on comparisons between GNR-GAPDH siRNA^{Cy3} nanoplexes and normal untreated control.

3. Results

3.1. Nanoplex formation

The cationic GNRs electrostatically complex to siRNA^{Cy3}, allowing for the study of the capacity of siRNA to interact with the nanoparticle surface (Figure 1A). The binding efficiency of siRNA^{Cy3} with GNRs was confirmed using agarose gel electrophoresis as described by Bonoiu et al., 2009 [22]. This data indicates the complexation of siRNA^{Cy3} with GNRs, with the highest loading of GNRs with siRNA calculated to be 17.5 μg/nmol. Further, confirmation of nanoplex formation is provided by the observation of a 5 nm shift in the longitudinal surface resonance peak of GNRs and by investigating the nanoplex aggregation using transmission electron microscopy (Figure 1B) [22]. The size of nanoplexes is estimated at 35 nm × 72 nm (width/length), and surface charge (zeta potential) measurements of free GNRs is +28.6 mV and upon complexation with siRNA is −2.4 mV. The nanoplexes remain stable for more than 1 month post-complexation [9].

3.2 *In vitro* cellular localization of nanoplexes

Prior to *in vivo* studies, we have demonstrated the capability of nanoplexes to deliver siRNA^{FAM} in DRG neurons. Dark field images of DRG neurons were generated by using plasmonic enhanced scattering from GNRs recorded after treatment with the nanoplex GNR-siRNA^{FAM} (500 ng GNR/nmol siRNA). The longitudinal surface plasmon oscillation of GNRs gives strong plasmonic scattering in the orange-red region of the optical spectrum (Figure 2, panels a and b). It is evident that nanoplexes are avidly taken up by DRG neurons (Figure 2). Interestingly, siRNA^{FAM} is not observed in DRG neurons in the absence of GNRs (Figure 2, panel i). The ability of GNRs to deliver siRNA^{FAM} in DRG neurons was compared with a lipid transfection reagent, X-tremeGENE, (Figure 2, compare panels c and f), and it was found that the GNR is a shuttle twice more efficient than the X-tremeGENE reagent (Figure 3). This experiment highlights an advantage of using nanotechnology in the delivery of therapeutics, where in addition to the therapeutic efficacy, the unique properties of the nanoparticles can be exploited in order to monitor the cellular entry/distribution of the nanoparticles using novel imaging techniques such as dark-field imaging with siRNA^{FAM}, either free, complexed with GNRs, or complexed with the commercially available transfection reagent X-tremeGENE.

To specifically determine the uptake and intracellular distribution of our nanoplexes, we performed TEM. A549 cells were treated with nanoplexes for 24 h and visualized by TEM. Figure 1C shows the presence of these nanoplexes inside the cells in an endosomal compartment [26].

3.3 Fluorescence studies from cell lysates

DRG cells incubated with free siRNA^{FAM} (1 nmol), GNR-siRNA^{FAM} (500 ng GNR/1 nmol siRNA^{FAM}), and X-tremeGENE-siRNA (5 μl X-tremeGene/1 nmol siRNA^{FAM}) nanoplexes were processed for fluorescence measurements 24 h later. The medium was removed and the cells were lysed using M-PER (mammalian protein extraction reagent; Pierce). The emission spectra of the cell lysates were collected using a Spectrofluorometer (Fluorolog®-3, Horiba Jobin Yvon). All the samples were dispersed in HPLC water and loaded into a quartz cell for measurements. Our results indicate that while lysates from cells treated with free siRNA^{FAM} show little or no fluorescence, the fluorescence from lysates of cells treated with GNR-siRNA^{FAM} is 1.48 units higher than that from cells treated with X-tremeGENE-siRNA^{FAM} (Figure 3) indicating that the intracellular delivery efficiency of siRNA using GNRs is superior to that using this commercially available gene transfection reagent (Figure 3). Whereas siRNA^{FAM} was used for the *in vitro* DRG neuron studies, siRNA^{Cy3} was used for the *in vivo* nanoplex studies as it is preferable to siRNA^{FAM} due to endogenous autofluorescence interference with detection of the FAM signal.

3.4. Nanoplex injection into the brain

A major obstacle to *in vivo* silencing is successful delivery of siRNA. In most *in vivo* studies using free siRNA, the resultant gene silencing is short-lived (1–3 days) and costly due to the necessity of multiple injections to deliver large amounts of siRNA to sustain the silencing [29, 37]. For example, 40% silencing of TNFα was achieved within 24 hours following direct injection of 0.05 nmols TNFα siRNA into the rat somatosensory cortex. The behavioral effect (EEG slow wave activity) of this silencing, however, was no longer apparent after 3 days [29, 37]. Likewise, continuous infusion into the mouse dorsal third ventricle of an siRNA targeting the dopamine transporter (0.4 mg/day for 14 days) resulted in significant hyper-locomotive effects by day-12 of the continuous infusion and widespread knockdown of dopamine transporter mRNA at day-14 [38]. To address the delivery issue, Pardridge (2007) [39] has shown that weekly administration of pegylated immunoliposome encapsulated siRNA can block gene expression in the brain. Since nanoparticles have successfully been used for *in vitro* delivery of siRNA into dorsal root ganglion cells (see Figure 2), we addressed this issue by using GNR-siRNA nanoplexes to silence the expression of the housekeeping gene GAPDH in the hippocampus *in vivo*. Figure 4 shows a representative bright-field and reflectance confocal image of nanoplexes (GNR-GAPDH siRNA^{Cy3}) 11 days after injection into the hippocampus. The reflectance image of the GNRs in the hippocampal section shows strong labeling with nanoplexes (green staining). Based on the number of particles visualized in this section using the reflectance method, this indicates the site of nanoplex injection into the CA1 region of the hippocampus.

3.5. *In vivo* cellular localization of nanoplexes

To determine the cell type(s) in which the uptake of the nanoplexes was associated *in vivo*, rat coronal hippocampal sections were labeled with primary antibodies to either glial fibrillary acidic protein (GFAP) (glial cells) or neurofilament-200 (NF-200) (neurons). Visualization of the primary antibody labeling was achieved using an IgG1-AlexaFluor 647 (AF-647) secondary antibody, with the excitation/emission maxima at 650/668 nm. The GNR-GAPDH-siRNA^{Cy3} nanoplex uptake into hippocampal cells was visualized in the same tissue sections, since the excitation/emission maxima of 514/566 nm for Cy3 provides emission in the yellow region of the spectrum and is well separated from the far-red (AF-647) fluorophore emission, thereby facilitating a multicolor analysis. An overlay of the respective images demonstrates co-localization of the GNR-GAPDH siRNA^{Cy3} nanoplexes with neurons (NF-200 positive), as opposed to glial cells (GFAP positive) (Figure 5). Figure 6 shows the cellular uptake of GNR-GAPDH-siRNA^{Cy3} in hippocampal cells after stereotaxic injection into the CA1 region of hippocampus [40]. The nanoplexes appear to

remain localized into the CA1 region, with little diffusion to adjacent regions, as staining is pronounced in the CA1 region when viewed across each of the coronal sections throughout the rostral half of the hippocampus. These results confirm that stereotactic injection allows for localization of the nanoplexes to desired/specific regions, as well as the uptake of the nanoplexes into cells of the hippocampus.

3.6. Knockdown of hippocampal GAPDH gene expression following injection of GNR-GAPDH siRNA^{Cy3} nanoplexes

The nanoplexes were administered into the CA1 region of the right hippocampus, and gene silencing was determined by measuring the percentage inhibition of the expression of GAPDH using quantitative real-time PCR (Q-RT-PCR). Results from these experiments show a >70% suppression of GAPDH gene expression in the CA1 region and in the combined CA3/dentate gyrus regions of the hippocampus at 4 days post-injection (n=3; Figure 7), and injection of GNR-scrambled siRNA^{Cy3} had no effect on GAPDH siRNA levels (data not shown). This level of suppression was maintained for up to 11 days post-injection (n=3; Figure 7), in comparison with injection of free siRNA. The brain region overlying the injection site, part of the parietal cortex, was used as a control region for diffusion, showing localization of the nanoplex-induced knockdown to the hippocampus. Thus, the GNR-siRNA produces a longer lasting knockdown that is less invasive and that may be critical in the assessment of functional/behavioral evidence of continued knockdown. Taken together, these results provide a solid foundation clearly supporting the hypothesis that GNRs complexed with siRNA can effectively and efficiently knockdown gene expression in select regions of the rat brain.

It is notable that the behavior and weights of the GAPDH knockdown rats were not different from those of control rats after targeting the hippocampus, suggesting that overall health of the animals was not affected by GNR uptake or by the gene knockdown.

3.7. *In vitro* siRNA release from GNR-siRNA nanoplexes

In order to determine the release kinetics of siRNA from the GNRs, brain microvascular endothelial cells (BMVEC) that are routinely cultured in our laboratory in numbers sufficient to perform these studies were transfected with GNR-GAPDH siRNA^{Cy3} (500 ng/nmol siRNA), and the amount of free siRNA^{Cy3} released into the cell was assessed. Briefly, 3×10^5 cells/ml were seeded in 35 mm dishes and transfected with the same nanoplex solution. The cells were lysed using M-PER reagent followed by centrifugation at 13,000 rpm for 5 minutes. The supernatants were collected, and the emission spectrum was measured using a Spectrofluorometer. The pellet was diluted in 1 ml PBS, and the emission spectrum of the solution was also acquired. We observed that siRNA^{Cy3} is released over time from the surface of GNRs. On day-1 post-transfection, 6% of the siRNA is released from the surface of GNRs as measured in the supernatant; 94% of the siRNA remains electrostatically coupled to the GNR surface as measured in the pellet (Figure 8A). Day-2 post-transfection, the level of siRNA elaborated into the cytoplasm increased to 40% (Figure 8B). After 6 days, only 5% of the siRNA remains coupled to the GNRs surface as per cell pellet measurement (data not shown), supporting the progressive release of the siRNA from the GNRs. A major obstacle to siRNA use in brain therapy is the need to continually perfuse the area of interest with the silencer as free siRNA is rapidly degraded in the cytoplasm of the cell. In this case, an advantage of siRNA delivery using GNRs is the protective effect of GNRs on silencer degradation especially as the continuous perfusion of the area of interest will be not necessary. We speculate the polyelectrolyte layers on the GNRs surface provide a “shielding effect”, protecting the siRNA that is in contact with the enzymes that cause the degradation.

4. Discussion

Delivery of drugs or biological compounds into the whole animal traditionally relies on the use of soluble substances or liposome-assisted transmembrane transport. Many biologically active compounds have a ubiquitous distribution and accumulate in a variety of cells, or multiple tissue locations, precluding specific accumulation entirely in targeted cells or tissue. Therefore, recent technological developments have led scientists to investigate the use of nanoparticle methodology for biomedical applications. This novel approach enables the site specific delivery of a compound, thereby reducing or eliminating the off-site delivery and subsequent unwanted detrimental responses.

The field of nanomedicine is rapidly advancing with the development of novel therapies based on gene delivery [5, 7, 13]. Gene silencing by RNA interference (using siRNA) is rapidly emerging as a powerful tool for inhibition of gene expression [13, 39]. The use of siRNA for knocking-down gene expression has evolved from the awareness that numerous disease states are a result of abnormal gene expression. Consequently, an increase or blockade of gene expression in specific cell populations would be therapeutically beneficial. However, some challenges need to be overcome before this technique can be applied for clinical trials. For example, problems of targeted delivery and instability of siRNA in the biological environment need to be overcome. In order to address these issues, several methods for delivering siRNA *in vivo* have been explored. Nevertheless, methods that are effective for peripheral organ delivery, such as electroporation and hydrodynamic injection of siRNA, are not applicable to brain delivery [41]. Furthermore, direct continuous infusion of free siRNA into the brain ventricular system induced gene knockdown that was widespread without selectivity to targeted brain regions [38, 42]. Specific targeting of brain regions by direct injection of siRNA has resulted in localized gene knockdown [43], but this knockdown is transient due to the rapid degradation of the siRNA [29].

In this study, we used GNRs for successful loading, delivery and release of siRNA molecules for housekeeping gene suppression in the rat hippocampus. The use of these nanoparticles brings major advantages for '*in vivo*' research. First, GNRs are biocompatible materials easy to load with siRNA molecules. The cellular toxicity of nanoplexes was assessed *in vitro* on DAN and A459 cells, and there was no significant toxicity detected [22,26]. Previous studies used viruses for direct injection of siRNA precursors (shRNA) into the brain [44]. However, safety issues regarding the possibility of conversion of the virus to a pathogenic form limit the use of this method clinically. Using GNRs as shuttles for siRNA delivery eliminates the problem of shuttle-induced toxicity in the biological host compared with other shuttles [44]. Second, the optical tracking properties of GNRs (SPR and reflectance) confirm the formation of the nanoplex *in vitro* and permit visualization of transfected nanoplexes by dark field microscopy (see Figures 2 and 4) [45]. Additionally, the GNR shape and surface allows for increased amount of silencer to be loaded on their surface improving the rate of siRNA transfected [22]. Third, the GNRs sustain, protect, and slowly release the siRNA. The delivery of GNR-siRNA successfully blocked GAPDH gene expression in the hippocampus that was long-lived (11 days) and elicited by a single injection of a relatively small amount of siRNA into the CA1 region of the rat hippocampus (see Figure 7). Recently, dendrimer-conjugated magnetofluorescent nanoworms, or "dendriworms", were used as a platform for intracranial siRNA delivery [3]. Whereas this study used a continuous microinfusion of siRNA carrying-dendriworms over a 3- or 7-day period to produce significant decreases in targeted protein levels, the present study shows the efficiency and power of a single injection of non-viral GNR-siRNA nanoplexes for generating sustained knockdown of endogenous gene expression in the adult rat brain. We speculate that slow release of the siRNA from the GNRs, as demonstrated *in vitro* (see

Figure 8), contributes to the sustained knockdown of gene expression in the hippocampus *in vivo*.

The occurrence of abnormal gene expression in the hippocampus is costly in many diseases, including depression, chronic pain, and Alzheimer's disease. Additionally, the anatomy of the hippocampus is conserved from mouse to human, providing translational relevance for experimental discoveries [46]. Because of its vital role in releasing selective proteins during diseases associated with the brain, we chose to target the hippocampus for the knockdown of a gene. We predict that by knocking-down representative gene expression in the hippocampus, numerous diseases could be prevented or controlled. Therefore, specific genes in the hippocampus are possible therapeutic targets to treat the central component of scores of brain disorders.

5. Conclusions

The integration of nanoscience and nanotechnology into biomedical research is ushering in a true revolution that is having a broad impact in biomedical science. However, the limited success in treating many neurological health problems may in part be due to difficulty in targeting therapy to selective brain regions. We hypothesized that GNR delivery of siRNA would allow for both regional and cell selective knockdown of targeted gene expression *in vivo*. GNRs are particularly attractive for therapeutic applications due to their biocompatibility and ease of complex formation with a variety of biomolecules (e.g. siRNA, DNA, etc.). GNRs offer stability and protection against degradation of the siRNA gene silencing molecules. These GNR-siRNA nanoplexes were shown to effectively and efficiently knockdown gene expression for a prolonged period of time. In conclusion, when comparing to traditional transfection agents and viral vectors, our GNRs provide more efficient delivery and target specificity to cells and are superior in protecting and stabilizing siRNA in the biological milieu, thereby resulting in a more prolonged half-life of the siRNA within target cells. These observations underscore the major benefits that nanotechnology can offer towards the safe and efficient delivery of siRNA based therapeutics to the brain and other privileged sites. Thus, this report of the *in vivo* use of GNR-siRNA nanoplexes is an encouraging step toward the application of nanoplexes for therapeutic gene knockdown in human subjects.

Acknowledgments

The authors wish to thank Dr. Charles M. Severin for the use of his stereotaxic apparatus.

References

1. Prasad, PN. Introduction to Biophotonics. Wiley-Interscience; New York: 2004.
2. Whitesides GM. Nanoscience, Nanotechnology, and Chemistry. Small. 2005; 1(2):172–179. [PubMed: 17193427]
3. Agrawal A, Min DH, Singh N, et al. Functional delivery of siRNA in mice using dendriworms. ACS Nano. 2009; 3(9):2495–2504. [PubMed: 19673534]
4. Ferrari M. Cancer nanotechnology: opportunities and challenges. Nat Rev Cancer. 2005; 5(3):161–171. [PubMed: 15738981]
5. Bharali DJ, Klejbor I, Stachowiak EK, et al. Organically modified silica nanoparticles: A nonviral vector for in vivo gene delivery and expression in the brain. Proc Natl Acad Sci USA. 2005; 102(32):11539–11544. [PubMed: 16051701]
6. Kang H, DeLong R, Fisher MH, Juliano RL. Tat-Conjugated PAMAM dendrimers as delivery agents for antisense and siRNA oligonucleotides. J Pharm Res. 2005; 22(12):2099–2106.

7. Klejbor I, Stachowiak EK, Bharali DJ, et al. ORMOSIL nanoparticles as a non-viral gene delivery vector for modeling polyglutamine induced brain pathology. J Neurosci Meth. 2007; 165(2):230–243.
8. Ghosh P, Han G, De M, Kim CK, Rotello VM. Gold nanoparticles in delivery applications. Adv Drug Deliv Rev. 2008; 60(11):1307–1315. [PubMed: 18555555]
9. Ding H, Yong K-T, Roy I, et al. Gold nanorords coathed with multilayer Polyelectrolyte as contrast agent for multimodal Imaging. J Phys Chem C. 2007; 34(111):12552–12557.
10. Huang X, Jain PK, El-Sayed IH, El-Sayed MA. Gold nanoparticles: interesting optical properties and recent applications in cancer diagnostics and therapy. Nanomedicine. 2007; 2(5):681–693. [PubMed: 17976030]
11. Bartlett DW, Davis ME. Effect of siRNA nuclease stability on the in vitro and in vivo kinetics of siRNA-mediated gene silencing. Biotechnology and Bioengineering. 2007; 97(4):909–921. [PubMed: 17154307]
12. Davis ME. The first targeted delivery of siRNA in humans via a self-assembling, cyclodextrin polymer-based nanoparticle: from concept to clinic. Mol Pharm. 2009; 6(3):659–668. [PubMed: 19267452]
13. Davis ME, Zuckerman JE, Choi CH, et al. Evidence of RNAi in humans from systemically administered siRNA via targeted nanoparticles. Nature. 2010; 464(7291):1067–1070. [PubMed: 20305636]
14. Li S-D, Huang L. Nanoparticles evading the reticuloendothelial system: role of the supported bilayer. Biochim Biophys Acta – Biomembranes. 2009; 1788:2259–2266.
15. Li J, Chen Y-C, Tseng Y-C, Mozumdar S, Huang L. Biodegradable calcium phosphate nanoparticle with lipid coating for systemic siRNA delivery. J Controlled Release. 2010; 142:416–421.
16. Hauck TS, Ghazani AA, Chan WC. Assessing the effect of surface chemistry on gold nanorod uptake, toxicity, and gene expression in mammalian cells. Small. 2008; 4(1):153–159. [PubMed: 18081130]
17. Yong K-T, Roy I, Ding H, Bergey EJ, Prasad PN. Biocompatible near-infrared quantum dots as ultrasensitive probes for long-term *in vivo* imaging applications. Small. 2009; 5(17):1997–2004. [PubMed: 19466710]
18. Roy I, Stachowiak MK, Bergey EJ. Non viral gene transfection nanoparticles: Functions and applications in CNS. Nanomedicine. 2008; 4(2):89–97. [PubMed: 18313990]
19. Connor EE, Mwamuka J, Gole A, Murphy CJ, Wyatt MD. Gold nanoparticles are taken up by human cells but do not cause acute cytotoxicity. Small. 2005; 1(3):325–327. [PubMed: 17193451]
20. Yu C, Naksharti H, Irudayaraj J. Identity profiling of cell surface markers by multiplex gold nanorod probes. Nano Letters. 2007; 7(8):2300–2306. [PubMed: 17602538]
21. Tan WB, Jiang S, Zhang Y. Quantum-dot based nanoparticles for targeted silencing of HER2/neu gene via RNA interference. Biomaterials. 2007; 28:1565–1571. [PubMed: 17161865]
22. Bonoiu AC, Mahajan SD, Ding H, et al. Nanotechnology approach for drug addiction therapy: Gene silencing using delivery of gold nanorod-siRNA nanoplex in dopaminergic neurons. Proc Natl Acad Sci USA. 2009; 106(14):5546–5550. [PubMed: 19307583]
23. Kang B, Mackey MA, El-Sayed MA. Nuclear targeting of gold nanoparticles in cancer cells induces DNA damage, causing cytokinesis arrest and apoptosis. J Am Chem Soc. 2010; 132(5): 1517–1519. [PubMed: 20085324]
24. Yong K-T, Sahoo Y, Swihart MT, Schneeberger PM, Prasad PN. Templated synthesis of gold nanorods (NRs): The effects of cosurfactants and electrolytes on the shape and optical properties. Top Catal. 2008; 47:49–60.
25. Nuwer MO, Picchione KE, Bhattacharjee A. cAMP-dependent kinase does not modulate the Slack sodium-activated potassium channel. Neuropharmacology. 2009; 57(3):219–226. [PubMed: 19540251]
26. Chakravarthy KV, Bonoiu AC, Davis WG, et al. Gold nanorod delivery of an ssRNA immune activator inhibits pandemic H1N1 influenza viral replication. Proc Natl Acad Sci USA. 2010; 107(22):10172–10177. [PubMed: 20498074]

27. Paxinos, G.; Watson, C. The rat brain in stereotaxic coordinates. 3. Academic Press; New York: 1997.
28. Qiu Y, Liu Y, Wang L, et al. Surface chemistry and aspect ratio mediated cellular uptake of Au nanorods. Biomaterials. 2010; 31(30):7606–7619. [PubMed: 20656344]
29. Taishi P, Churchill L, Wang M, et al. TNF[alpha] siRNA reduces brain TNF and EEG delta wave activity in rats. Brain Res. 2007; 1156:125–132. [PubMed: 17531209]
30. Ignatowski TA, Noble BK, Wright JR, et al. Neuronal-associated tumor necrosis factor (TNF[alpha]): its role in noradrenergic functioning and modification of its expression following antidepressant drug administration. J Neuroimmunol. 1997; 79(1):84–90. [PubMed: 9357451]
31. Javier DJ, Nitin N, Levy M, Ellington A, Richards-Kortum R. Aptamer-targeted gold nanoparticles as molecular-specific contrast agents for reflectance imaging. Bioconjugate Chemistry. 2008; 19(6):1309–1312. [PubMed: 18512972]
32. Hu R, Yong K-T, Roy I, Ding H, He S, Prasad PN. Metallic nanostructures as localized plasmon resonance enhanced scattering probes for multiplex dark field targeted imaging of cancer cells. J Phys Chem C Nanomater Interfaces. 2009; 113(7):2676–2684. [PubMed: 20046993]
33. Yong K-T, Swihart MT, Ding H, Prasad PN. Preparation of gold nanoparticles and their applications in anisotropic nanoparticle synthesis and bioimaging. Plasmonics. 2009; 4(2):79–93.
34. Chomczynski P, Sacchi N. Single-step method of RNA isolation by acid guanidinium thiocyanate-phenol-chloroform extraction. Anal Biochem. 1987; 162(1):156–159. [PubMed: 2440339]
35. Radonić A, Thulke S, Mackay IM, Landt O, Siegert W, Nitsche A. Guideline to reference gene selection for quantitative real-time PCR. Biochem Biophys Res Commun. 2004; 313(4):856–862. [PubMed: 14706621]
36. Bustin SA. Quantification of mRNA using real-time reverse transcription PCR (RT-PCR): trends and problems. J Mol Endocrinol. 2002; 1(29):23–39. [PubMed: 12200227]
37. Fu AL, Yan XB, Sui L. Down-regulation of [beta]1-adrenoceptors gene expression by short interfering RNA impairs the memory retrieval in the basolateral amygdala of rats. Neurosci Lett. 2007; 428(2–3):77–81. [PubMed: 17961922]
38. Thakker DR, Natt F, Hüsken D, et al. Neurochemical and behavioral consequences of widespread gene knockdown in the adult mouse brain by using nonviral RNA interference. Proc Natl Acad Sci USA. 2004; 101(49):17270–17275. [PubMed: 15569935]
39. Pardridge WM. shRNA and siRNA delivery to the brain. Advanced Drug Delivery Reviews. 2007; 59(2–3):141–152. [PubMed: 17434235]
40. Bjarkam CR, Pedersen M, Sørensen JC. New strategies for embedding, orientation and sectioning of small brain specimens enable direct correlation to MR-images, brain atlases, or use of unbiased stereology. J Neurosci Meth. 2001; 108(2):153–159.
41. Leung RK, Whittaker PA. RNA interference: From gene silencing to gene-specific therapeutics. Pharmacol Ther. 2005; 107(2):222–239. [PubMed: 15908010]
42. Thakker DR, Weatherspoon MR, Harrison J, et al. Intracerebroventricular amyloid-β antibodies reduce cerebral amyloid angiopathy and associated micro-hemorrhages in aged Tg2576 mice. Proc Natl Acad Sci USA. 2009; 106(11):4501–4506. [PubMed: 19246392]
43. Hoyer D. RNA interference for studying the molecular basis of neuropsychiatric disorders. Curr Opin Drug Discov Devel. 2007; 10(2):122–129.
44. Mahairaki V, Xu L, Farah MH, et al. Targeted knock-down of neuronal nitric oxide synthase expression in basal forebrain with RNA interference. J Neurosci Meth. 2009; 179(2):292–299.
45. Chen C-D, Cheng S-F, Chau L-K, Wang CRC. Sensing capability of the localized surface plasmon resonance of gold nanorods. Biosens Bioelectron. 2007; 22:926–932. [PubMed: 16697633]
46. Cryan JF, Holmes A. The ascent of mouse: advances in modelling human depression and anxiety. Nat Rev Drug Discov. 2005; 4(9):775–790. [PubMed: 16138108]

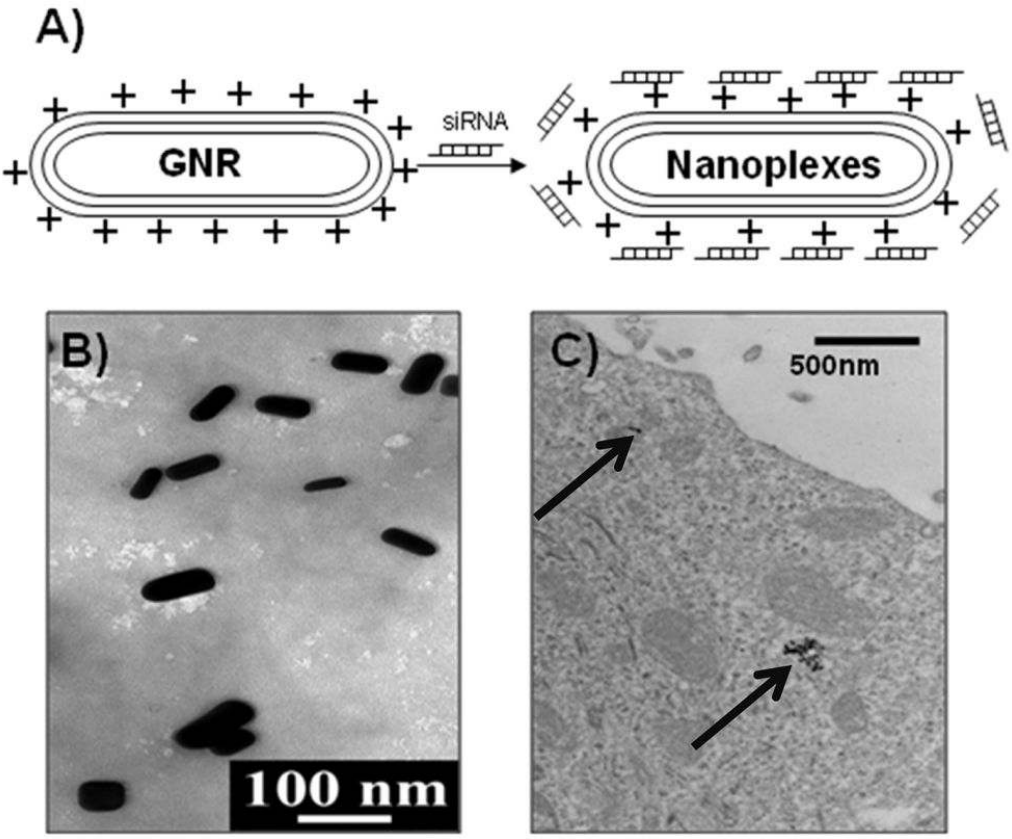

Figure 1.
GNR-siRNA nanoplex formation. A) Schematic presentation of nanoplex formation. Cationic coated GNRs electrostatically couple with negatively charged siRNA to form stable nanoplexes. B) Transmission electron microscopy (TEM) image of GNR-siRNA nanoplexes. Distribution of GNRs shows no sign of aggregation upon complexation with siRNA. Nanoplex size is estimated at width (35 nm) × length (72 nm). C) Cellular uptake of nanoplexes following internalization into A549 cells as visualized using TEM. Nanoplexes are seen at the cell periphery within uncoated tubules and vacuoles. Under higher magnification, the particles are observed to be internalized within the different endocytic compartments.

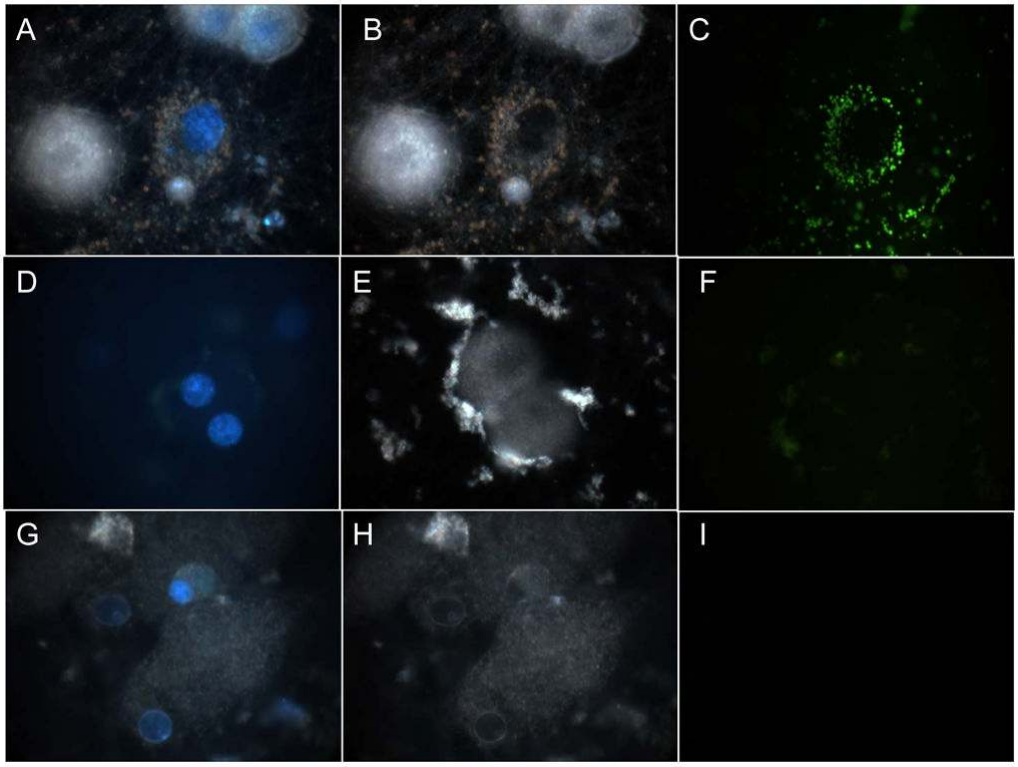

Figure 2.

Nanoplex uptake in dorsal root ganglion (DRG) cells. The cellular uptake and distribution of the nanoplex GNR-siRNA^{FAM} in DRG cells was demonstrated using dark field and fluorescence microscopy. The siRNA^{FAM} from the nanoplex is detected in the fluorescence field (green), and additional nuclear staining (blue, Hoechst) was performed. Panels **A** and **B** show the dark-field images of DRG cells treated with the GNR-siRNA nanoplex. The intracellular delivery of the nanoplexes can be easily observed from the strong orange-red scattering of GNRs from the nanoplex in dark field. Panel **C** shows green fluorescence distribution of siRNA from the nanoplex. Comparison of siRNA^{FAM} delivery into these cells using GNRs was to the commercially available gene silencing agent X-tremeGENE (Panels **D**, **E**, and **F**). Free siRNA^{FAM} is not taken up by the DRG neurons (Panels **G**, **H**, and **I**). The samples containing DRG neurons transfected with GNR-siRNA^{FAM} were excited by a pulsed diode laser at 405 and 488 nm (PDL800-D, PicoQuant GmbH); the photomultiplier tube 1 (PMT1) was set with filter of 450–550 nm. Same magnification (60X objective) used for all pictures.

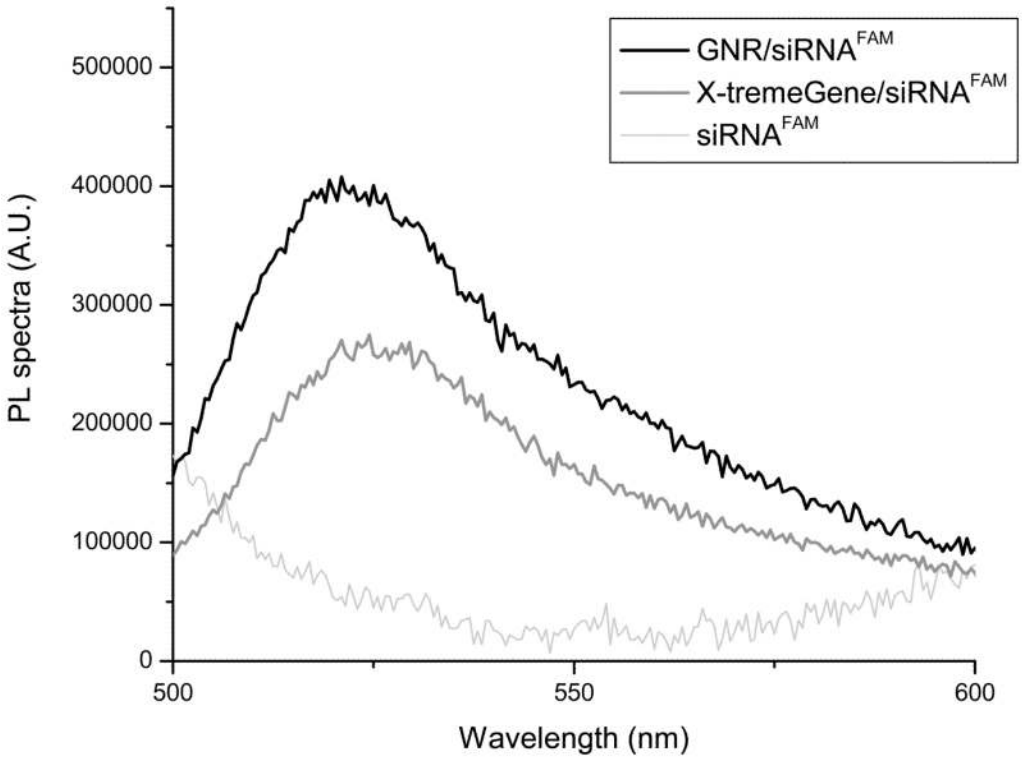

Figure 3.

Quantitative expression of transfection efficiency in DRG neurons. Fluorescence spectra of siRNA^{FAM} taken from lysates of DRG cells after transfection using GNR-siRNA^{FAM} nanoplexes, X-tremeGENE-siRNA^{FAM} complexes, and free siRNA^{FAM}. Data shows that transfection with the GNR-siRNA^{FAM} nanoplexes results in the highest cellular uptake. Data is representative of duplicate experiments.

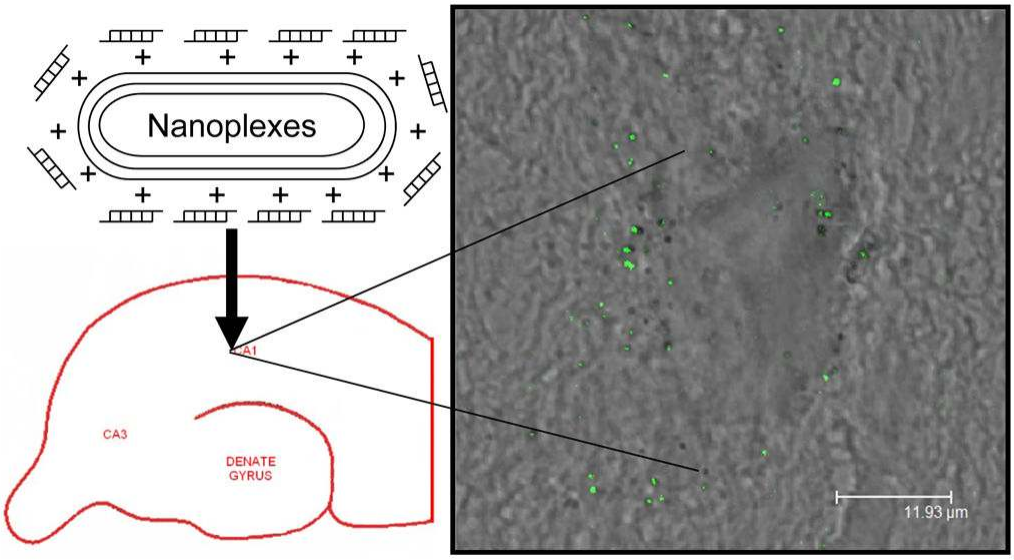

Figure 4.

Reflectance imaging of GNR-GAPDH siRNA^{Cy3} nanoplexes. Nanoplex distribution in the rat hippocampus was determined by monitoring GNR reflectance after nanoplex injection. In this bright-field confocal image, GNR reflectance is represented by green dots.

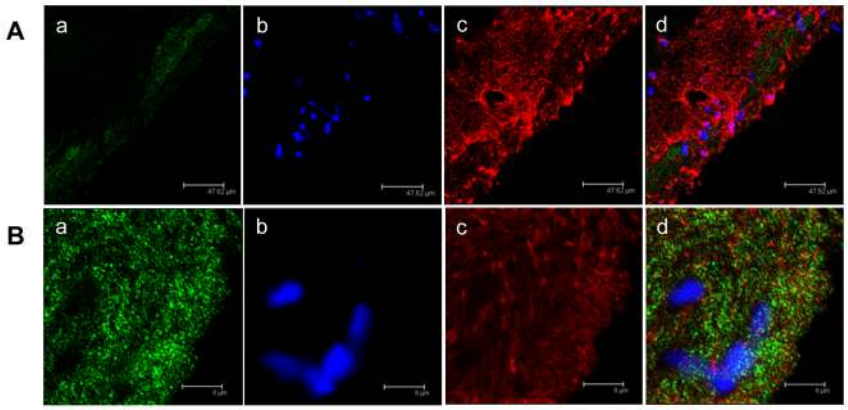

Figure 5.

Immunofluorescent labeling showing nanoplex distribution in rat coronal hippocampal sections. GNR-GAPDH siRNA^{Cy3} was injected into the CA1 region of the hippocampus. The hippocampi were isolated 24 hr later and frozen tissue sections were prepared. Identification of cell type was by immunofluorescent staining (10 μm section, acetone-fixed). **Rows A and B**: Visualization of GNR-GAPDH siRNA^{Cy3} staining (panel a, green); nuclear (Hoechst dye, 10μM)) blue staining (panel b); Glial fibrillary acidic protein, GFAP (1:30,000, Sigma-Aldrich) staining for glial cells (Row **A**, panel c) or Neurofilament-200, NF-200 (1:30,000, Sigma) staining for neurons (Row **B**, panel c) using goat anti-mouse IgG1-AlexaFluor 647 (1:2,000, Invitrogen) secondary antibody (red), and (panel d) overlay of images showing co-localization. Data is representative of three replicate experiments.

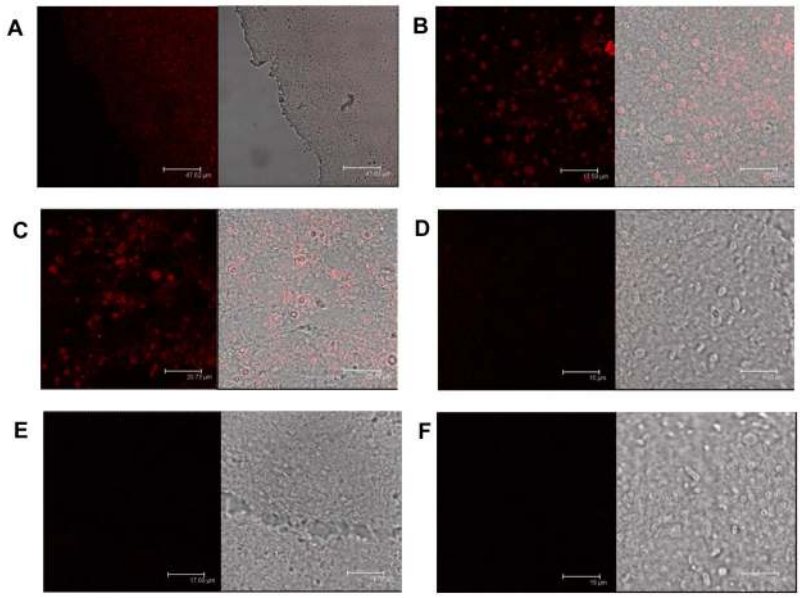

Figure 6.

Nanoplex distribution in rat hippocampus. Confocal microscopic images of the CA1 region in the rat right hippocampus 24 hr after injection (6 μl; 0.5 μl/min) of nanoplex GNR-GAPDH siRNA^{Cy3} (500 ng/1 nmol). Coronal hippocampal sections (10 μm, unfixed) were imaged using confocal microscopy: the dark (left) panel displays GNR-siRNA^{Cy3} distribution in fluorescence images and the light (right) panel shows overlay of fluorescence and transmission images. Fluorescence (Cy3) labeling of the siRNA was visualized with a 590 nm filter. (**A**) A representative rostral section (from sections #2–4) shows siRNA incorporation into hippocampal cells, evident at higher (**B**) magnification. (**C**) A representative field taken from sections #37–40 demonstrates siRNA^{Cy3} staining. (**D**) A field from sections #57–60 shows negligible staining for siRNA^{Cy3} (the staining is visible only in overlay transmission imagines). (**E**) Staining is no longer evident in sections #77–80, approximately half-way through the hippocampus. (**F**) Left hippocampal tissue served as the negative control; injection of GNRs alone results in absence of staining; injection of GAPDH siRNA^{Cy3} alone demonstrates staining that is of less intensity and more diffuse (not cellularly localized). Data is representative of three separate experiments.

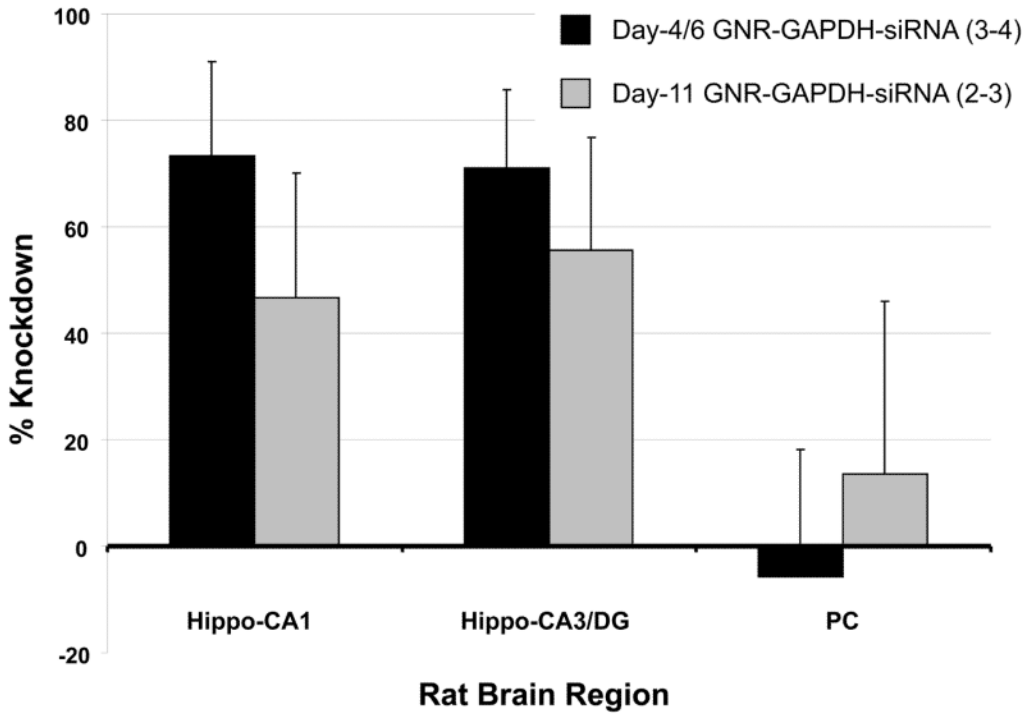

Figure 7.

Knockdown of GAPDH gene expression using GNR-GAPDH siRNA^{Cy3} in the rat hippocampus. A single injection (6 μl; 0.5 μl/min) of GNR-GAPDH siRNA^{Cy3} (500 ng/1 nmol) was administered into the CA1 region of the right hippocampus (or GNR-scrambled siRNA^{Cy3} for comparison purposes). The Q-RT-PCR data shows >70% suppression of GAPDH gene expression in the CA1 region and in the combined CA3/dentate gyrus regions of the right hippocampus at 4 days post-injection. This level of suppression was maintained for up to 11 days post-injection. The brain region overlying the injection site, part of the parietal cortex, was used as a control region for diffusion. Results are expressed as the mean ± SEM with the *n* number indicated in parentheses. As published, binding of siRNA with GNRs and loading efficiency was monitored by agarose gel electrophoresis mobility [22]. Hippo, hippocampus; DG, dentate gyrus; PC, parietal cortex.

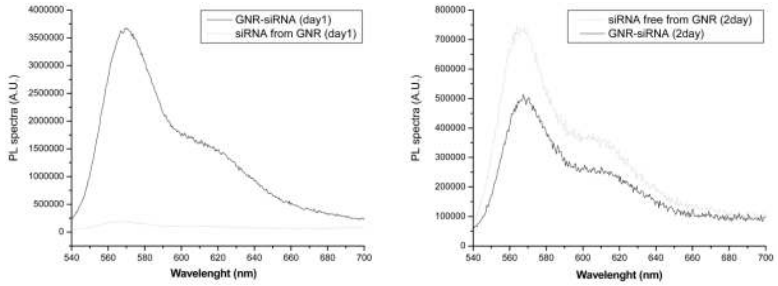

Figure 8.

Release kinetics of siRNA from GNRs. Brain microvascular endothelial cells (BMVEC) loaded with nanoplex GNR-siRNA^{Cy3} were monitored for two days to evaluate the release of siRNA^{Cy3} into the cytoplasm. Both GNR-siRNA^{Cy3} nanoplexes and free siRNA^{Cy3} (released from GNRs) were assessed at: (A) day 1 and (B) day 2 post-transfection by measuring the emission at 590 nm. Data is representative of duplicate experiments.